Published in final edited form as:
Neurochem Res. 2012 July ; 37(7): 1490–1498. doi:10.1007/s11064-012-0740-2.

Bilateral common carotid artery ligation transiently changes brain lipid metabolism in rats

Abesh Kumar Bhattacharjee[1,+], **Laura White**[1], **Lisa Chang**[1], **Kaizong Ma**[1], **G. Jean Harry**[2], **Joseph Deutsch**[1,3], and **Stanley I. Rapoport**[1,*]

[1]Brain Physiology and Metabolism Section, National Institute on Aging, National Institutes of Health, Bethesda, MD, USA

[2]Neurotoxicology Group, National Institute of Environmental Health Sciences, National Institutes of Health, Research Triangle Park, NC, USA

[3]The Hebrew University of Jerusalem, School of Pharmacy, Jerusalem, Israel

Abstract

Brain lipid metabolism was studied in rats following permanent bilateral common carotid artery ligation (BCCL), a model for chronic cerebral hypoperfusion. Unesterified (free) fatty acids (uFA) and acyl-CoA concentrations were measured 6 h, 24 h, and 7 days after BCCL or sham surgery, in high energy-microwaved brain. In BCCL compared to sham rats, $cPLA_2$ immunoreactivity in piriform cortex, and concentrations of total uFA and arachidonoyl-CoA, an intermediate for arachidonic acid reincorporation into phospholipids, were increased only at 6 h. At 24 h, immunoreactivity for secretory phospholipase A_2 ($sPLA_2$), which may regulate blood flow, was increased near cortical and hippocampal blood vessels. BCCL did not affect difference brain IB_4+ microglia, glial fibrillary acidic protein (GFAP)+ astrocytes, cyclooxygenase-2 (COX-2) immunoreactivity at any time, but increased cytosolic $cPLA_2$ immunoreactivity in one region at 6 h. Thus, BCCL affected brain lipid metabolism transiently, likely because of compensatory $sPLA_2$-mediated vasodilation, without producing evidence of neuroinflammation.

Keywords

arachidonic acid; ischemia; carotid; ligation; acyl-CoA; brain; $cPLA_2$; $sPLA_2$; rat; brain; neuroinflammation

Introduction

The brain has a high demand for oxidation of glucose for the synthesis of adenosine triphosphate (ATP), and pathological changes occur when oxygen delivery is chronically impaired [1–3]. Reduction of cerebral blood flow (CBF) limits oxygen delivery and causes cerebral ischemia. Chronic CBF reduction is major cause of vascular dementia [4–6], which accounts for approximately 20% of age related dementias [4]. Low CBF also is considered an aggravating factor for Alzheimer disease [7], and for dementia associated with sleep apnea [8]. In Alzheimer disease and vascular dementia, the severity and persistence of cerebral hypoperfusion correlate with the severity of cognitive impairment [9–11].

*Address Correspondence to: Stanley I. Rapoport, M.D. Brain Physiology and Metabolism Section, National Institute on Aging, National Institutes of Health, 9000 Rockville Pike, Bethesda, MD, 20892 USA. Tel: 301 496 1765; Fax: 301 402 0074; sir@helix.nih.gov.
+**Current address:** Psychiatry Residency Program, U.C. San Diego, Department of Psychiatry, 9500 Gillman Drive #9116A, La Jolla, CA 92093

Complete interference of the carotid or vertebro-basilar circulation in rodents has identified vulnerability of specific brain regions, including the hippocampus and frontal cortex [12, 13]. While the severity of brain damage following acute CBF reduction is well established, less is known about effects of chronic CBF insufficiency. Permanent occlusion of both common carotid arteries in the rat (bilateral common carotid artery ligation (BCCL)) has been used as an experimental model for chronic cerebral hypoperfusion [14]. After BCCL, CBF immediately declines to 30–60% of its control value, but recovers to approximately ~63% and ~90% of control at four- and eight-weeks, respectively [15, 16].

BCCL in the rat produced neuronal loss in the hippocampus and cerebral cortex [17–20], and altered brain carbohydrate metabolism, high-energy phosphates, neurotransmitters and behavior [21–26]. These effects may result from decreased oxidative metabolism and decreased synthesis of ATP following reduced oxygen delivery to the brain [18, 27]. About 25% of net brain ATP consumption is accounted for by lipid metabolism [28]. Disruption of brain lipid metabolism secondary to reduced blood and oxygen flow, as well as reduced ATP production, also can have far reaching consequences.

In gerbils, which lack posterior communicating arteries between the carotid and vertebro-basilar circulations, BCCL produces complete forebrain ischemia, resulting in massive release of unesterified fatty acids (uFA) within 5 min and an increase in the concentration of arachidonyl (ARA)-CoA [29–31]. BCCL in rats may not produce as severe changes, however, since the rat has posterior communicating arteries.

One early study reported that brain concentrations of palmitic, stearic, oleic, ARA and docosahexaenoic acids were increased after decapitation at 6 h after BCCL [32]. However, it now is recognized that decapitation itself markedly distorts brain lipid concentrations through activation of lipases that release fatty acids from phospholipids, and that high energy microwaving can reduce this distortion [31, 33]. Because of the relevance of chronic partially reduced CBF to human brain disease (see above), in this paper we thought it important to measure concentrations, in high-energy microwaved brain of the rat, of long-chain unesterified fatty acids (uFAs) and acyl-CoAs, intermediates for reincorporation of released uFAs into phospholipids [34, 35], at different times following BCCL, or after sham operation. Since phospholipases A_2 (PLA_2) and cyclooxygenase (COX)-2 are involved in the metabolism of arachidonic acid (ARA) and docosahexaenoic acid [36–38], which are released during ischemia [39], we also used immunochemistry to examine regional brain COX-2 and PLA_2 proteins.

Methods

Chemicals

HPLC grade isopropanol was purchased from EM Science (Gibbstown, NJ, USA). Ammonium sulfate and acetic acid glacial were purchased from Mallinckrodt (Paris, KY, USA). Reagent grade methanol was from Mallinckrodt (Phillipsburg, NJ, USA). HPLC grade acetonitrile was obtained from Fisher Scientific (Fairlawn, NJ, USA). Potassium monobasic phosphate and acyl-CoA standards were from Sigma-Aldrich (St. Louis, MO, USA). Sodium pentobarbital was purchased from Richmond Veterinary Supply Co. (Richmond, VA, USA).

Animals

Male Wistar-Kyoto rats, aged 2–3 months and weighing 180–281 g (Charles River Laboratories, Wilmington, MA, USA), were maintained on a 12-h/12-h light/dark cycle in a temperature- and humidity-controlled facility with food and water available ad libitum. Rats were anesthetized with sodium pentobarbital (50 mg/kg, i.p) and both common carotid

arteries were exposed through a ventral cervical U-shaped incision. The arteries were separated from their sheaths and vagal nerves, and permanently ligated with 4-0 silk sutures. Sham animals underwent the same surgical procedure but without the actual ligation. All procedures were conducted under a protocol (#05-023) approved by the NICHD Animal Care and Use Committee in accordance with the Guide for the Care and Use of Laboratory Animals (NIH Publication 86-23).

To examine the time course of responses to BCCL, brains were collected at 6 h, 24 h and 7 days after BCCL or sham surgery. Rats (n = 6–10 per group at each time point) were anesthetized with sodium pentobarbital and immediately killed by focused high energy beam irradiation (5.4 kW, 3.8 sec, Cober Electronics, Stamford, CT, U.S.A.) [31]. The brain was excised and regions posterior to the posterior communicating arteries were discarded. The forebrain was bisected in the midsagittal plane and stored at −80 °C. One hemisphere was used for uFA analysis and the contralateral hemisphere for long chain acyl-CoA analysis. For histology, rats (n = 3–5 for each group at each time point) were deeply anesthetized with pentobarbital (50 mg/kg body wt), and transcardially perfused with 100 ml cold saline followed by 4% paraformaldehyde in PBS.

Brain lipid extraction and chromatography

Total lipids were extracted by the method of Folch [40]. The extracts were separated by thin layer chromatography on silica gel 60 plates (Whatman, Clifton, NJ, USA). uFAs were separated using a mixture of heptane (Fisher Scientific, Fair Lawn, NJ, USA): diethyl ether : glacial acetic acid (60:40:2 by volume) [41]. uFAs and standard bands were visualized with 6-p-toluidine-2-naphthalene-sulfonic acid (Acros, Fairlawn, NJ USA) under ultraviolet light. uFA bands were scraped and heptadecanoic acid (17:0) was added as an internal standard prior to extraction and methylation. Fatty acid methyl esters were prepared by heating the removed bands in 1% H_2SO_4 in methanol at 70°C for 3 hours [42]. The methyl esters were separated on a 30 m × 0.25 mm i.d. capillary column (SP-2330, Supelco; Bellefonte, PA, USA) using gas chromatography with a flame ionization detector (Model 6890N, Agilent Technologies; Palo Alto, CA, USA). Runs were initiated at 80 °C with a temperature gradient to 160° C (10° C/min) and 230° C (3° C/min) in 31 min and held at 230 °C for 10 min. Peaks were identified by retention times of fatty acid methyl ester standards (Nu-Chek-Prep, Elysian, MN, USA). Fatty acid concentrations (nmol/g brain) were calculated by proportional comparison of gas chromatography peak areas to that of the 17:0 internal standards.

Analysis of Acyl-CoA

Samples (0.3–0.4 g) plus 25 μl of 17:0 and 14:0- CoA as internal standards were placed on ice in a scintillation vial or a 15-ml conical vial prior to sonication. Then 25 mM KH_2PO_4 (2 ml) was added and sonicated for one min (output control 3 units). Isopropanol (2 ml) was added to the vial and the homogenate was sonicated again for 20 sec. Saturated ammonium sulphate (0.25 ml) was added and the sample was lightly shaken by hand. Acetonitrile (4 ml) was added and the sample was vortexed for 2 min prior to centrifugation. The upper phase was separated and 12 ml of 25 mM potassium phosphate was added. Each sample was run through an activated oligonucleotide purification cartridge (Applied Biosystems, Foster City, CA USA), washed with 1 ml of 25 mM potassium hydrogen phosphate (KH_2PO_4), and eluted with 200 μl isopropanol: 30 mM glacial acetic acid (75:25 by volume). The first 3 drops were discharged and the remaining 150 μl were collected in an auto sampler vial. Acyl-CoA species were separated using HPLC (Beckman-Coulter, Fullerton, CA, USA) with a Symmetry C-18, 5-μm column (250 × 4.6 mm; Waters-Millipore, Mildford, MA, USA) and UV absorbance was measured at 260 and 280 nm with a System Gold, 168 dual wavelength detector. Conditions were set to a 1 ml/min gradient system composed of (A) 75

mM KH_2PO_4 and (B) 100% acetonitrile. The gradient started with 44% B, then increased to 49% B over 25 min, and then to 68% B over 10 min. It remained at 68% B for an additional 5 min, then returned to 44% over 2 min and held for 8 min. Concentrations of acyl-CoA species (nmol/g wet weight) were identified according to the retention times of authentic standards and were measured using peak area analysis (32 Karat, version 5.0, Beckman Coulter) from HPLC chromatograms. A representative HPLC pattern of acyl-CoA concentrations in both sham (A) and BCCL (B) rat brains is shown in Figure 1. The peaks at 18 and 37 min represent internal standards of tetradecanoyl-CoA and heptadecanoyl-CoA (20 μl of each), respectively.

Histology

Following cardiac perfusion, brains were excised then post-fixed *in situ* for 6 h, bisected in the mid-sagittal plane, rinsed with PBS, dehydrated in ethanol, and embedded in paraffin. Serial 8-μm sections of the entire sagittal plane containing the hippocampus were collected, and from this pool of sections for each animal were randomly selected representing multiple planes of cut. Deparaffinized, rehydrated sections were treated to quench endogenous peroxidase and subjected to heat-induced epitope retrieval using a decloaking chamber (Biocare Medical, Walnut Creek, CA, USA). Microglia were detected by binding of *Griffonia simplicifolia* isolectin B_4 (IB_4; Sigma) at a 1:75 dilution in 1X Automation Buffer (AB; Biomedia Corp, Foster City, CA, USA) containing 0.1 M $CaCl_2$, $MgCl_2$, $MnCl_2$, and 0.1% Triton X-100 overnight at 4 °C. For immunohistochemistry, sections were blocked with avidin-biotin followed by 10% normal goat serum/ 1% BSA/ 1X AB. Astrocytes were identified with a rabbit polyclonal anti-glial fibrillary acidic protein (GFAP; 1:1000 for 30 min; Dako, Carpinteria, CA, USA) detected with an HRP labeled streptavidin–biotin kit. Sections were incubated with anti-secretory $sPLA_2$ or anti-cytosolic $cPLA_2$ (1:100; overnight at 4 °C; Santa Cruz) or anti-COX-2 polyclonal antibodies (1:1500; 1 h RT; Cayman Chemicals, Ann Arbor, MI, USA) detected by avidin biotin technique. Antigen retrieval was not used for anti-$cPLA_2$. Reaction products were visualized by 3,3′-diaminobenzidine (DAB) substrate. Sections were counterstained with modified Harris hematoxylin. Digital images of the entire brain section were acquired with a Leica DMRBE microscope (Wetzlar, Germany) or using the Aperio Scanscope T2 Scanner (Aperio Technologies, Vista, CA USA) and viewed using Aperio Imagescope v. 6.25.0.1117.

Statistics

Data are presented as mean ± standard deviation. Statistical significance was determined by a Student's *t*-test at each individual time point, with significance set at $p < 0.05$ as indicated by *, BCCL *vs.* sham.

Results

Unesterified fatty acids (uFAs)

Table 1 presents measured concentrations of brain uFAs at different times following BCCL or sham operation. At 6 h, there was a statistically significant increase in the concentration of DHA and of total uFAs compared to sham control ($p < 0.05$). At 24 h and 7 days, there was no significant difference in the concentration of total or any individual uFA between groups.

Acyl-CoAs

As illustrated in Table 2, the brain concentration of ARA-CoA at 6 h after BCCL was increased 2-fold, compared to its concentration in the sham rats. There was no group difference in any acyl-CoA concentration at 24 h or 7 days after BCCL.

Immunochemistry

A general histopathological evaluation of brain sections indicated no overt cell death in any region within the sagittal plane of cut as a result of BCCL. When scanning the entire plane of cut, specific staining by each antibody was detected in some brain regions. Immunoreactive product for COX-2 was detected in neurons within the somatosensory cortex (Figs. 1a,b), the piriform cortex (Figs. 1c,d), and CA3 pyramidal neurons of the hippocampus (Figs. 1e,f). Staining was similar in the BCCL rats and sham controls across all time points.

At 6 h, the general staining pattern involving $cPLA_2$ within the cortex was similar across the BCCL rats and sham controls (Fig. 2). In both groups, cytosolic $cPLA_2$ was detected in cell bodies and in processes of cerebellar Purkinje neurons, dentate granule cells, and cortical neurons. When matched for location and plane of cut, immunoreactive processes in the piriform cortex at 6 h after ligation displayed a more distinct staining pattern, suggesting upregulation, in BCCL compared with sham rats (Figs. 2c,d). This appeared to be a transient change, as no difference in staining pattern was seen at the 24-h or 7-day time points (data not shown).

In sham controls, secretory $sPLA_2$ was not detected and only rarely was a positive area detected in sections from the BCCL rats. This occurred only at the 24 h time point, within cells displaying a glia-type morphology suggestive of astrocytes, in close proximity to blood vessels in the cortex (data not shown). Also affected were the area between the dentate gyrus and the stratum lucidem (Fig. 3a), and the lacunosum molecular layer of the hippocampus (Fig. 3b). No immunopositive staining for $sPLA_2$ was evident in the brain parenchyma at the later 7-day time point.

The morphology and distribution of IB_4+ microglia and GFAP+ astrocytes in the hippocampus and cortex were similar between BCCL rats and sham controls. The overall staining for GFAP+ astrocytes in the hippocampus did not differ between BCCL and sham controls at any time point examined. IB_4 staining for microglia indicated no significant difference between BCCL and sham controls over time (data not shown).

Discussion

In the current study, an early indication of cerebral hypoperfusion was seen at 6 h after BCCL, as a statistically significant increase in the brain concentrations of total uFA, docosahexaenoic acid and ARA-CoA, the intermediate for reincorporation of unesterified ARA into brain phospholipids [29, 30, 34, 43]. $cPLA_2$ immunoreactivity appeared elevated in neuronal processes of the piriform cortex. These changes were absent at later times. At 24 h however, immunochemistry showed that $sPLA_2$ clearly was overexpressed close to blood vessels in the BCCL rats. The transient nature of the responses suggests that the uFAs released during BCCL were cleared within 24 h [29, 44].

Our mean sham-surgery uFA concentrations were comparable to reported values in microwaved rat or uFA [30, 31], but they had much larger variances than reported, as did concentrations following BCCL (Table 1). Possible causes for their increased variance are incomplete microwaving and modification by the sham operation itself, since our analytical methods were the same as used in the prior publications. The high variance limits information gathered from the uFA data, but might be overcome in future studies by using more animals [30, 31].

Our sham acyl-CoA concentrations also were comparable to published values in microwaved brain [30, 31]. The net acyl-CoA concentration was not changed significantly

by BCCL, which also was found following complete ischemia [30, 31]. This constancy may be due to binding of intracellular acyl-CoA to acyl-CoA binding proteins or acyl-CoA synthetases, whose availability is not changed by ischemia [45, 46]. As after 6 h of BCCL (Table 2), ARA-CoA was the only acyl-CoA elevated by complete ischemia or decapitation in other studies using microwaved brain [30, 31]. This elevation likely mediates increased energy-dependent reincorporation of unesterified ARA into phospholipid [29].

The increased total brain uFA concentration at 6 h after BCCL is consistent with a report elevated concentrations at 2, 4 and 6 h after BCCL, when the brain was removed after decapitation without microwaving [32]. However, the magnitude of the increase in our study at 6 h (1.55 fold) is much lower than in the prior study (11.3 fold) [32], likely because we used focused beam high energy microwaving of the brain before removing it, to denature brain fatty acid releasing enzymes [31, 33].

In gerbils, which lack posterior communicating arteries, increased brain concentrations of palmitic, stearic, oleic, linoleic, ARA and docosahexaenoic acids were reported at 5 min after BCCL, when the brain was subjected to high energy microwaving [30]. The total uFA concentration was increased by 4.4 fold at 5 min, much higher than the 1.55 fold increase in rats at 6 h after BCCL. The lack of posterior communication arteries results in complete forebrain ischemia in gerbils following BCCL [30].

This study revealed a significant increase in ARA-CoA, but no significant change in other acyl-CoA species at 6 h after BCCL, and no change in any acyl-CoA including ARA-CoA at 24 h (Table 2). These results suggest upregulated ARA reincorporation into brain at 6 h after BCCL. In complete ischemia in the gerbil, a high brain ARA-CoA concentration was associated with a higher ARA concentration. A high concentration of unesterified ARA can be neurotoxic, by interfering with cell signaling, gene transcription, mitochondrial oxidative phosphorylation, cell growth and excitability, and inducing apoptosis [47–49].

The transient nature of the brain response to BCCL was evidenced by the focal expression of $sPLA_2$ in close proximity to blood vessels at 24 h but not later, and evidence for increased $cPLA_2$ immunoreactivity. The perivascular location of $sPLA_2$ suggests a role in vasodilatation in the initial stages of BCCL, associated with formation of the potent ARA-derived vasodilator, prostaglandin E_2 (PGE_2) [50]. The transient nature of the response suggests that selective changes were induced on cerebral microvessels, which were not maintained over time. While there was no observed morphological response in microglia in the initial 24 h after BCCL, activated microglia as well as other pathological changes in gray and white matter have been noted 13 weeks after BCCL in rats [14, 51].

COX-2 is constitutively expressed in the brain in discrete neuronal populations. In the current study, COX-2 expression in neurons was not obviously different between BCCL and sham rats after 24 h (Fig. 2). With complete ischemia [50], lipopolysaccharide-induced neuroinflammation [52, 53], COX-2 was rapidly upregulated and promoted formation of pro-inflammatory eicosanoids like prostaglandin E_2 (PGE_2) [54–56].

Acute BCCL in rats leads to a transient cerebral hypoxia, which increases intracellular calcium [57] to activate ARA-selective $cPLA_2$ and release ARA and increase ARA recycling in phospholipid [58]. Activation of $sPLA_2$ by calcium [59] also may release ARA and ultimately to produce PGE_2 [50] to mediate compensatory vasodilatation. Nitric oxide, free radicals and neurogenic factors during ischemia also can produce vasodilatation [60, 61]. CBF recovers to ~63% and ~90% of its control value at 4 and 8 weeks after BCCL [14–16]. It is likely that some recovery occurred in the present study even at 24 h, associated with the $sPLA_2$ activation (Fig. 3), helping to normalize the significant disturbances in uFA and ARA-CoA concentrations evident at 6 h (Tables 1 and 2). However, autoregulation

remains abnormal and the brain is more vulnerable to additional insults such as hypotension, hypoxia and further ischemia following BCCL[62].

In conclusion, BCCL in rats caused an acute statistically significant increases in the net brain uFA concentration and the ARA-CoA concentration at 6 h, immunohistochemical evidence increased $cPLA_2$ expression in neuronal processes of the piriform cortex at 6 h and of $sPLA_2$ expression surrounding blood vessels at 24 h, suggesting vasodilation. These results demonstrate the transient nature of the brain metabolic response, likely because of the intervention of compensatory vasodilation over time. The absence of increased immunoreactivity for COX-2, IB_4+ microglia or GFAP+ astrocytes in the hippocampus and cortex in BCCL compared with sham control rats indicates that BCCL did not initiate significant neuroinflammation. Thus, BCCL exerts a low-threshold reversible ischemic brain insult, which transiently increases brain ARA metabolism and enzymes, but may increase vulnerability to further stress.

Acknowledgments

This research was supported entirely by the Intramural Research Program of the National Institute on Aging, and by the National Institute of Environmental Health Science, NIH.

Abbreviations

ARA	arachidonic acid
BCCL	bilateral common carotid artery ligation
$cPLA_2$	cytoplasmic phospholipase A_2
$sPLA_2$	secretory phospholipase A_2
CBF	cerebral blood flow
COX-2	cyclooxygenase 2
HRP	horseradish peroxidase
IB_4	isolectin B_4
GFAP	glial fibrillary acidic protein
uFA	unesterified fatty acid
PGE_2	prostaglandin E_2

References

1. de la Torre JC. How do heart disease and stroke become risk factors for Alzheimer’s disease? Neurol Res. 2006; 28:637–644. [PubMed: 16945216]
2. Kalaria RN. The role of cerebral ischemia in Alzheimer’s disease. Neurobiol Aging. 2000; 21:321–330. [PubMed: 10867217]
3. Siesjö, BK. Brain Energy Metabolism. John Wiley & Sons; Chichester: 1978. p. 1-607.
4. Kalaria RN, Kenny RA, Ballard CG, Perry R, Ince P, Polvikoski T. Towards defining the neuropathological substrates of vascular dementia. J Neurol Sci. 2004; 226:75–80. [PubMed: 15537525]
5. Napoli C, Palinski W. Neurodegenerative diseases: insights into pathogenic mechanisms from atherosclerosis. Neurobiol Aging. 2005; 26:293–302. [PubMed: 15639306]
6. Hachinski V, Munoz D. Vascular factors in cognitive impairment--where are we now? Ann N Y Acad Sci. 2000; 903:1–5. [PubMed: 10818482]

7. Esposito G, Giovacchini G, Liow JS, Bhattacharjee AK, Greenstein D, Schapiro M, Hallett M, Herscovitch P, Eckelman WC, Carson RE, Rapoport SI. Imaging neuroinflammation in Alzheimer's disease with radiolabeled arachidonic acid and PET. J Nucl Med. 2008; 49:1414–1421. [PubMed: 18703605]
8. Roman GC. Vascular dementia prevention: a risk factor analysis. Cerebrovasc Dis. 2005; 20(Suppl 2):91–100. [PubMed: 16327258]
9. Andin U, Gustafson L, Passant U, Brun A. A clinico-pathological study of heart and brain lesions in vascular dementia. Dement Geriatr Cogn Disord. 2005; 19:222–228. [PubMed: 15695924]
10. Scheel P, Puls I, Becker G, Schoning M. Volume reduction in cerebral blood flow in patients with vascular dementia. Lancet. 1999; 354:2137. [PubMed: 10609827]
11. Komatani A, Yamaguchi K, Sugai Y, Takanashi T, Kera M, Shinohara M, Kawakatsu S. Assessment of demented patients by dynamic SPECT of inhaled xenon-133. J Nucl Med. 1988; 29:1621–1626. [PubMed: 3262723]
12. Niedermeyer E. Alzheimer disease: caused by primary deficiency of the cerebral blood flow. Clin EEG Neurosci. 2006; 37:175–177. [PubMed: 16929700]
13. Swan JH, Evans MC, Meldrum BS. Long-term development of selective neuronal loss and the mechanism of protection by 2-amino-7-phosphonoheptanoate in a rat model of incomplete forebrain ischaemia. J Cereb Blood Flow Metab. 1988; 8:64–78. [PubMed: 2828386]
14. Farkas E, Luiten PG, Bari F. Permanent, bilateral common carotid artery occlusion in the rat: a model for chronic cerebral hypoperfusion-related neurodegenerative diseases. Brain Res Rev. 2007; 54:162–180. [PubMed: 17296232]
15. Kunimatsu T, Asai S, Kanematsu K, Kohno T, Misaki T, Ishikawa K. Effects of glutamate receptor agonist on extracellular glutamate dynamics during moderate cerebral ischemia. Brain Res. 2001; 923:178–186. [PubMed: 11743986]
16. Otori T, Katsumata T, Katayama Y, Terashi A. Measurement of regional cerebral blood flow and glucose utilization in rat brain under chronic hypoperfusion conditions following bilateral carotid artery occlusion. Analyzed by autoradiographical methods. Nippon Ika Daigaku Zasshi. 1997; 64:428–439. [PubMed: 9366147]
17. Institoris A, Farkas E, Berczi S, Sule Z, Bari F. Effects of cyclooxygenase (COX) inhibition on memory impairment and hippocampal damage in the early period of cerebral hypoperfusion in rats. Eur J Pharmacol. 2007; 574:29–38. [PubMed: 17719573]
18. de la Torre JC, Cada A, Nelson N, Davis G, Sutherland RJ, Gonzalez-Lima F. Reduced cytochrome oxidase and memory dysfunction after chronic brain ischemia in aged rats. Neurosci Lett. 1997; 223:165–168. [PubMed: 9080458]
19. Ni JW, Matsumoto K, Li HB, Murakami Y, Watanabe H. Neuronal damage and decrease of central acetylcholine level following permanent occlusion of bilateral common carotid arteries in rat. Brain Res. 1995; 673:290–296. [PubMed: 7606443]
20. Nanri M, Miyake H, Murakami Y, Matsumoto K, Watanabe H. Chronic cerebral hypoperfusion-induced neuropathological changes in rats. Nihon Shinkei Seishin Yakurigaku Zasshi. 1998; 18:181–188. [PubMed: 10028489]
21. Tanaka K, Wada-Tanaka N, Miyazaki I, Nomura M, Ogawa N. Chronic cerebral hypoperfusion induces striatal alterations due to the transient increase of NO production and the depression of glutathione content. Neurochem Res. 2002; 27:331–336. [PubMed: 11958536]
22. Otori T, Katsumata T, Muramatsu H, Kashiwagi F, Katayama Y, Terashi A. Long-term measurement of cerebral blood flow and metabolism in a rat chronic hypoperfusion model. Clin Exp Pharmacol Physiol. 2003; 30:266–272. [PubMed: 12680845]
23. Liu HX, Zhang JJ, Zheng P, Zhang Y. Altered expression of MAP-2, GAP-43, and synaptophysin in the hippocampus of rats with chronic cerebral hypoperfusion correlates with cognitive impairment. Brain Res Mol Brain Res. 2005; 139:169–177. [PubMed: 15964096]
24. Farkas B, Tantos A, Schlett K, Vilagi I, Friedrich P. Ischemia-induced increase in long-term potentiation is warded off by specific calpain inhibitor PD150606. Brain Res. 2004; 1024:150–158. [PubMed: 15451377]

25. Schmidt-Kastner R, Aguirre-Chen C, Saul I, Yick L, Hamasaki D, Busto R, Ginsberg MD. Astrocytes react to oligemia in the forebrain induced by chronic bilateral common carotid artery occlusion in rats. Brain Res. 2005; 1052:28–39. [PubMed: 16023090]
26. Liu D, Wu L, Breyer R, Mattson MP, Andreasson K. Neuroprotection by the PGE2 EP2 receptor in permanent focal cerebral ischemia. Ann Neurol. 2005; 57:758–761. [PubMed: 15852374]
27. Lu J, Tong XY, Wang XL. Altered gene expression of Na+/Ca2+ exchanger isoforms NCX1, NCX2 and NCX3 in chronic ischemic rat brain. Neurosci Lett. 2002; 332:21–24. [PubMed: 12377375]
28. Purdon, AD.; Rapoport, SI. Energy consumption by phospholipid metabolism in mammalian brain. In: Gibson, G.; Dienel, G., editors. Neural Energy Utilization: Handbook of Neurochemistry and Molecular Biology. Vol. 16. Springer; New York: 2007. p. 401-427.
29. Rabin O, Chang MC, Grange E, Bell J, Rapoport SI, Deutsch J, Purdon AD. Selective acceleration of arachidonic acid reincorporation into brain membrane phospholipid following transient ischemia in awake gerbil. J Neurochem. 1998; 70:325–334. [PubMed: 9422378]
30. Rabin O, Deutsch J, Grange E, Pettigrew KD, Chang MC, Rapoport SI, Purdon AD. Changes in cerebral acyl-CoA concentrations following ischemia-reperfusion in awake gerbils. J Neurochem. 1997; 68:2111–2118. [PubMed: 9109539]
31. Deutsch J, Rapoport SI, Purdon AD. Relation between free fatty acid and acyl-CoA concentrations in rat brain following decapitation. Neurochem Res. 1997; 22:759–765. [PubMed: 9232626]
32. Kuwashima J, Nakamura K, Fujitani B, Kadokawa T, Yoshida K, Shimizu M. Relationship between cerebral energy failure and free fatty acid accumulation following prolonged brain ischemia. Jpn J Pharmacol. 1978; 28:277–287. [PubMed: 691873]
33. Murphy EJ. Brain fixation for analysis of brain lipid-mediators of signal transduction and brain eicosanoids requires head-focused microwave irradiation: an historical perspective. Prostaglandins Other Lipid Mediat. 2010; 91:63–67. [PubMed: 19660569]
34. Robinson PJ, Noronha J, DeGeorge JJ, Freed LM, Nariai T, Rapoport SI. A quantitative method for measuring regional in vivo fatty-acid incorporation into and turnover within brain phospholipids: Review and critical analysis. Brain Research Reviews. 1992; 17:187–214. [PubMed: 1467810]
35. Sun GY, MacQuarrie RA. Deacylation-reacylation of arachidonoyl groups in cerebral phospholipids. Ann N Y Acad Sci. 1989; 559:37–55. [PubMed: 2672943]
36. Ong WY, Sandhya TL, Horrocks LA, Farooqui AA. Distribution of cytoplasmic phospholipase A2 in the normal rat brain. J Hirnforsch. 1999; 39:391–400. [PubMed: 10536872]
37. Pardue S, Rapoport SI, Bosetti F. Co-localization of cytosolic phospholipase A2 and cyclooxygenase-2 in Rhesus monkey cerebellum. Brain Res Mol Brain Res. 2003; 116:106–114. [PubMed: 12941466]
38. Shimizu T, Wolfe LS. Arachidonic acid cascade and signal transduction. J Neurochem. 1990; 55:1–15. [PubMed: 2113081]
39. Bazán NG. Arachidonic acid in the modulation of excitable membrane function and at the onset of brain damage. Annals of the New York Academy of Sciences. 1989; 559:1–16.
40. Folch J, Lees M, Sloane Stanley GH. A simple method for the isolation and purification of total lipides from animal tissues. J Biol Chem. 1957; 226:497–509. [PubMed: 13428781]
41. Skipski VP, Good JJ, Barclay M, Reggio RB. Quantitative analysis of simple lipid classes by thin-layer chromatography. Biochim Biophys Acta. 1968; 152:10–19. [PubMed: 4296328]
42. Makrides M, Neumann MA, Byard RW, Simmer K, Gibson RA. Fatty acid composition of brain, retina, and erythrocytes in breast- and formula-fed infants. Am J Clin Nutr. 1994; 60:189–194. [PubMed: 7913291]
43. Rapoport SI. Arachidonic acid and the brain. J Nutr. 2008; 138:2515–2520. [PubMed: 19022981]
44. Rabin O, Drieu K, Grange E, Chang MC, Rapoport SI, Purdon AD. Effects of EGb 761 on fatty acid reincorporation during reperfusion following ischemia in the brain of the awake gerbil. Mol Chem Neuropathol. 1998; 34:79–101. [PubMed: 9778647]
45. Coleman RA, Lewin TM, Van Horn CG, Gonzalez-Baro MR. Do long-chain acyl-CoA synthetases regulate fatty acid entry into synthetic versus degradative pathways? The Journal of nutrition. 2002; 132:2123–2126. [PubMed: 12163649]

46. Knudsen J, Neergaard TB, Gaigg B, Jensen MV, Hansen JK. Role of acyl-CoA binding protein in acyl-CoA metabolism and acyl-CoA-mediated cell signaling. The Journal of nutrition. 2000; 130:294S–298S. [PubMed: 10721891]
47. Bazan NG, Rodriguez de Turco EB. Membrane lipids in the pathogenesis of brain edema: phospholipids and arachidonic acid, the earliest membrane components changed at the onset of ischemia. Adv Neurol. 1980; 28:197–205. [PubMed: 6779509]
48. Kovalchuk Y, Miller B, Sarantis M, Attwell D. Arachidonic acid depresses non-NMDA receptor currents. Brain Res. 1994; 643:287–295. [PubMed: 7518328]
49. Surette ME, Krump E, Picard S, Borgeat P. Activation of leukotriene synthesis in human neutrophils by exogenous arachidonic acid: inhibition by adenosine A(2a) receptor agonists and crucial role of autocrine activation by leukotriene B(4). Mol Pharmacol. 1999; 56:1055–1062. [PubMed: 10531413]
50. Li RC, Row BW, Gozal E, Kheirandish L, Fan Q, Brittian KR, Guo SZ, Sachleben LR Jr, Gozal D. Cyclooxygenase 2 and intermittent hypoxia-induced spatial deficits in the rat. Am J Respir Crit Care Med. 2003; 168:469–475. [PubMed: 12773326]
51. Farkas E, Donka G, de Vos RA, Mihaly A, Bari F, Luiten PG. Experimental cerebral hypoperfusion induces white matter injury and microglial activation in the rat brain. Acta Neuropathol (Berl). 2004; 108:57–64. [PubMed: 15138777]
52. Rosenberger TA, Villacreses NE, Hovda JT, Bosetti F, Weerasinghe G, Wine RN, Harry GJ, Rapoport SI. Rat brain arachidonic acid metabolism is increased by a 6-day intracerebral ventricular infusion of bacterial lipopolysaccharide. J Neurochem. 2004; 88:1168–1178. [PubMed: 15009672]
53. Lee H, Villacreses NE, Rapoport SI, Rosenberger TA. In vivo imaging detects a transient increase in brain arachidonic acid metabolism: a potential marker of neuroinflammation. J Neurochem. 2004; 91:936–945. [PubMed: 15525347]
54. Marcheselli VL, Bazan NG. Sustained induction of prostaglandin endoperoxide synthase-2 by seizures in hippocampus. Inhibition by a platelet-activating factor antagonist. J Biol Chem. 1996; 271:24794–24799. [PubMed: 8798751]
55. Kaufmann WE, Andreasson KI, Isakson PC, Worley PF. Cyclooxygenases and the central nervous system. Prostaglandins. 1997; 54:601–624. [PubMed: 9373877]
56. Miettinen S, Fusco FR, Yrjanheikki J, Keinanen R, Hirvonen T, Roivainen R, Narhi M, Hokfelt T, Koistinaho J. Spreading depression and focal brain ischemia induce cyclooxygenase-2 in cortical neurons through N-methyl-D-aspartic acid-receptors and phospholipase A2. Proc Natl Acad Sci U S A. 1997; 94:6500–6505. [PubMed: 9177247]
57. Farooqui AA, Horrocks LA. Excitatory amino acid receptors, neural membrane phospholipid metabolism and neurological disorders. Brain Res Brain Res Rev. 1991; 16:171–191. [PubMed: 1662102]
58. Clark JD, Schievella AR, Nalefski EA, Lin LL. Cytosolic phospholipase A2. J Lipid Mediat Cell Signal. 1995; 12:83–117. [PubMed: 8777586]
59. Dennis EA. Diversity of group types, regulation, and function of phospholipase A2. J Biol Chem. 1994; 269:13057–13060. [PubMed: 8175726]
60. Bolanos JP, Almeida A. Roles of nitric oxide in brain hypoxia-ischemia. Biochim Biophys Acta. 1999; 1411:415–436. [PubMed: 10320673]
61. Rodrigo J, Fernandez AP, Serrano J, Peinado MA, Martinez A. The role of free radicals in cerebral hypoxia and ischemia. Free Radic Biol Med. 2005; 39:26–50. [PubMed: 15925277]
62. Irikura K, Morii S, Miyasaka Y, Yamada M, Tokiwa K, Yada K. Impaired autoregulation in an experimental model of chronic cerebral hypoperfusion in rats. Stroke. 1996; 27:1399–1404. [PubMed: 8711809]

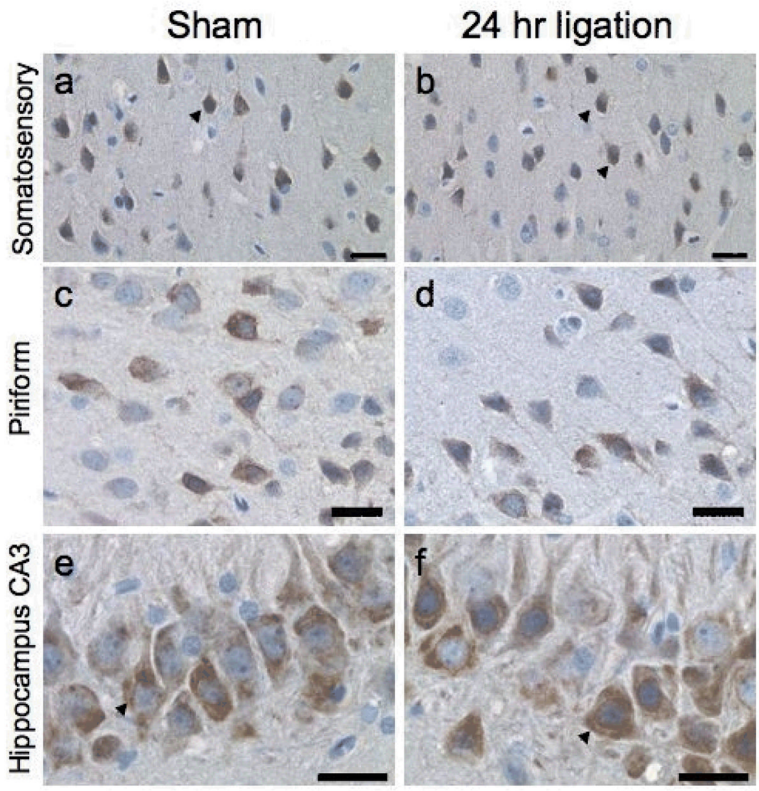

Figure 1.

Representative immunohistochemical staining for COX-2 at 24 h after BCCL or sham operation. The sagittal plane of cut for the full section of the brain was scanned using an Aperio Scanscope T2 Scanner and viewed with an Aperio Imagescope. Staining was evident only in neurons within the somatosensory cortex (a,b), the piriform cortex (c,d), and the CA-3 pyramidal cell layer (e,f) at 24 h after ligation (b,d,f) or in sham controls (a,c,e). Neuronal staining for COX-2 was visualized by DAB and had primarily a cytoplasmic distribution (arrow). Hematoxylin counterstained. Scale bar = 25 microns

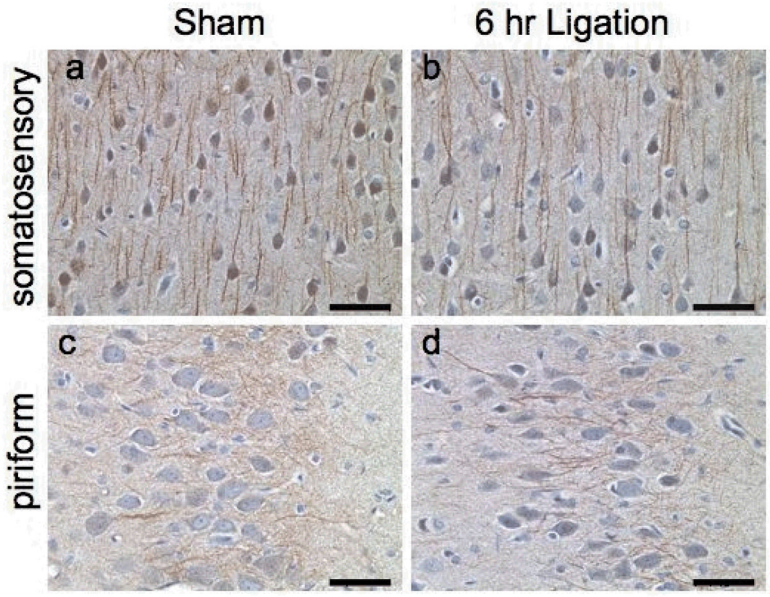

Figure 2.

Representative immunohistochemical staining for $cPLA_2$ at 6 h in the cortex as visualized by DAB. Within the entire plane of cut of the brain, scanning with an Aperio Scanscope indicated positive staining in neurons and neuronal processes only within the somatosensory cortex (a,b) and the piriform cortex (c,d). Neuronal cell body and processes showed positive staining in both the sham (a,c) and ligated (b,d) rats at the 6 h time point. Neurons in the piriform cortex displayed distinct processes 6 h after BCCL (d) compared to sham controls (c). Hematoxylin counterstain. Scale bar = 50 microns.

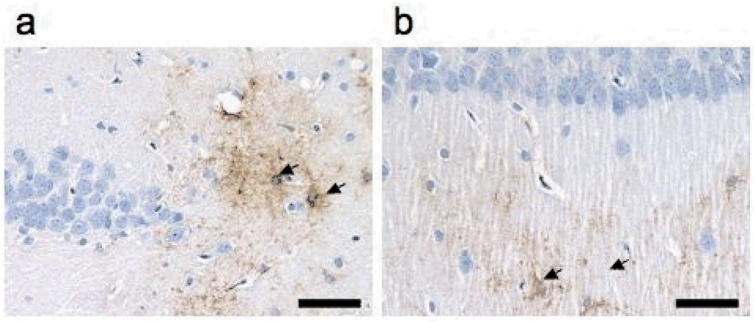

Figure 3.

Representative immunohistochemical staining for $sPLA_2$ in the hippocampus at 24 h after BCCL. Immunopositive cells visualized by DAB (arrows) displayed a glia like morphology and were evident in the (a) area between the dentate gyrus and the stratum lucidem and the (b) lacunosum moleculare layer. Hematoxylin counterstain. Scale bar = 50 microns

Table 1

Unesterified fatty acid concentrations in brain from BCCL and sham treated rats at different time points.

Time		Palmitate 16:0	Stearate 18:0	Oleate 18:1n-9	Linoleate 18:2n-6	Arachidonate 20:4n-6	Docosahexaenoate 22:6n-3	Total
				nmol/g				
6h	BCCL (n= 10)	51.6±41.6	89.2±42.1	19.3±7.2	14.5±18.4	14.4±11.7	13.3±5.1*	202.4±63.9*
	Sham (n= 10)	32.6±20.3	62.5±17.5	15.6±6.7	4.2±1.3	7.7±4.6	7.6±6.9	130.1±50.1
24h	BCCL (n= 7)	49.5±47.5	62.4±22.6	18.2±8.0	8.5±9.2	10.0±5.6	11.0±9.1	159.6±60.1
	Sham (n= 7)	50.0±46.9	66.9±32.3	17.4±7.0	8.0±9.3	10.5±6.8	12.3±12.2	165.1±65.0
7day	BCCL (n=8)	27.1±11.0	66.8±26.6	27.1±13.8	12.3±9.7	10.8±6.2	23.4±31.0	165.9±69.5
	Sham (n= 6)	36.7±21.4	46.9±10.6	22.5±11.2	9.8±8.4	8.0±2.6	9.2±3.6	133.2±41.6

Data represent the mean ± SD,

* $p < 0.05$ significantly different from sham by Student's t-test.

Table 2

Acyl-CoA concentrations in brain from BCCL and sham rats at different times

Time		Palmitate 16:0	Stearate 18:0	Oleate 18:1n-9	Linoleate 18:2n-6	Arachidonate 20:4n-6	Docosahexaenoate 22:6n-3	Total
Concentration, nmol/g								
6 h	BCCL (n=7)	10.43±0.39	3.51±0.63	9.40±0.96	0.69±0.36	2.18±1.13 *	1.71±0.52	27.98±2.39
	Sham (n=7)	10.29±0.72	2.90±0.74	9.13± 0.93	0.52±0.14	1.10±0.52	1.50±0.45	25.59±2.49
24 h	BCCL (n=6)	12.95±1.13	3.20±0.35	11.82±0.92	0.63±0.17	1.18± 0.31	1.36±0.35	30.54±1.77
	Sham (n=6)	13.11±1.05	3.06±0.46	11.78±0.98	0.54±0.06	0.92± 0.17	1.14±0.39	30.54±2.89

Data are mean ± SD.

* significantly different from sham, Student's t-test, $p < 0.05$.